Chemical and NADH-Induced, ROS-Dependent, Cross-Linking between Subunits of Complex I from *Escherichia coli* and *Thermus thermophilus*[†]

John M. Berrisford,[‡] Christopher J. Thompson,[‡] and Leonid A. Sazanov*

Medical Research Council Dunn Human Nutrition Unit, Wellcome Trust/MRC building, Hills Road, Cambridge CB2 0XY, U.K.

Received June 20, 2008; Revised Manuscript Received August 4, 2008

ABSTRACT: Complex I of respiratory chains transfers electrons from NADH to ubiquinone, coupled to the translocation of protons across the membrane. Two alternative coupling mechanisms are being discussed, redox-driven or conformation-driven. Using "zero-length" cross-linking reagent and isolated hydrophilic domains of complex I from *Escherichia coli* and *Thermus thermophilus*, we show that the pattern of cross-links between subunits changes significantly in the presence of NADH. Similar observations were made previously with intact purified *E. coli* and bovine complex I. This indicates that, upon reduction with NADH, similar conformational changes are likely to occur in the intact enzyme and in the isolated hydrophilic domain (which can be used for crystallographic studies). Within intact *E. coli* complex I, the cross-link between the hydrophobic subunits NuoA and NuoJ was abolished in the presence of NADH, indicating that conformational changes extend into the membrane domain, possibly as part of a coupling mechanism. Unexpectedly, in the absence of any chemical cross-linker, incubation of complex I with NADH resulted in covalent cross-links between subunits Nqo4 (NuoCD) and Nqo6 (NuoB), as well as between Nqo6 and Nqo9. Their formation depends on the presence of oxygen and so is likely a result of oxidative damage *via* reactive oxygen species (ROS) induced cross-linking. In addition, ROS- and metal ion-dependent proteolysis of these subunits (as well as Nqo3) is observed. Fe-S cluster N2 is coordinated between subunits Nqo4 and Nqo6 and could be involved in these processes. Our observations suggest that oxidative damage to complex I *in vivo* may include not only side-chain modifications but also protein cross-linking and degradation.

Complex I (NADH:ubiquinone oxidoreductase, EC 1.6.5.3) is the first enzyme of the mitochondrial and bacterial respiratory chains. It catalyzes the transfer of two electrons from NADH to quinone, coupled to the translocation of approximately four protons across the membrane, contributing to the protonmotive force required for the synthesis of ATP (*1, 2*). The mitochondrial enzyme is one of the largest known membrane protein complexes, consisting of 45 different subunits (*3*) with a combined molecular mass of about 980 kDa. The prokaryotic enzyme (also referred to as NDH-1) is simpler and consists of between 13 and 15 subunits with a total mass of about 550 kDa (*2, 4*). Analogues of all conserved subunits of bacterial complex I are found within the mitochondrial enzyme (*1*), and they both contain equivalent redox components (*2*). The mitochondrial and bacterial enzymes have similar characteristic L-shaped structure, with the hydrophobic arm embedded in the membrane and the hydrophilic peripheral arm protruding into the mitochondrial matrix or the bacterial cytoplasm (*5*−*8*). Thus, the bacterial enzyme can be considered to represent a "minimal" model of complex I. Because of the central role of complex I in respiration, mutations in individual subunits can lead to many human neurodegenerative diseases (*9*). Also, along with complex III (bc_1), complex I has been suggested to be a major source of reactive oxygen species (ROS)[1] in mitochondria, which can damage mitochondrial DNA and may be one of the causes of aging (*10*). Parkinson's disease, at least in its sporadic form (which represents about 95% of cases), may be caused by increased ROS production from malfunctioning complex I (*11*).

In contrast to most other membrane protein complexes of the respiratory chain, the atomic structure of the entire complex I is not yet known (*12*). Relatively low resolution electron microscopy studies have revealed an L-shape in all species studied so far (*5*−*7, 13, 14*). The hydrophilic domain, or peripheral arm, of complex I contains the NADH binding site and all known redox centers: the primary electron acceptor flavin mononucleotide (FMN) and eight to nine iron−sulfur (Fe-S) clusters (*2, 15, 16*). Therefore, all electron transfer events before quinone reduction are likely to happen in this domain. We have previously determined the crystal structure of the hydrophilic domain of complex I from *Thermus thermophilus*, establishing the electron transfer pathway from the FMN, located near the tip of the peripheral arm, to the quinone binding site at the interface with the

[†] This research was funded by the Medical Research Council.

* To whom correspondence should be addressed. Tel: +44 1223 252910. Fax: +44 1223 252915. E-mail: sazanov@mrc-dunn.cam.ac.uk.

[‡] These authors contributed equally to the manuscript.

[1] Abbreviations: Bis-Tris, 2-bis(2-hydroxyethyl)amino-2-(hydroxymethyl)-1,3-propanediol; DDM, *n*-dodecyl β-D-maltoside; DTT, dithiothreitol; EDC, 1-ethyl-3-(3-dimethylaminopropyl)carbodiimide hydrochloride; EEDQ, *N*-(ethoxycarbonyl)-2-ethoxy-1,2-dihydroquinoline; HEPES, 4-(2-hydroxyethyl)-1-piperazineethanesulfonic acid; OG, *n*-octyl β-D-glucoside; ROS, reactive oxygen species; sulfo-SMCC, *N*-sulfosuccinimidyl 4-(*N*-maleimidomethyl)cyclohexane-1-carboxylate.

10.1021/bi801160u CCC: $40.75
Published on Web 09/05/2008

membrane domain (*17*). The atomic structure of the membrane-spanning part of the enzyme is not yet known. It seemingly lacks prosthetic groups, but it must contain essential components of the proton translocating machinery. Sequence comparisons have suggested that the largest hydrophobic subunits of complex I, NuoL, NuoM, and NuoN (*Escherichia coli* nomenclature), are homologous to each other and that they have evolved from a common ancestor related to the K^+ or Na^+/H^+ antiporter family (Mrp) (*18*−*20*). Therefore, these subunits are likely to participate in proton translocation.

Although electron transfer events in the hydrophilic domain are now relatively well understood (*12*), the mechanism of coupling between electron transfer and proton pumping remains unknown. Two different models are being discussed: direct (redox-driven, employing modifications of the Q cycle or another chemical intermediate) (*21*) and indirect or conformation-driven coupling (*2, 22*−*25*). There is no experimental data yet to support the first model (*26*), although some features of the structure of the hydrophilic domain can be interpreted as consistent with it (*17*). These include, for example, the unique coordination of terminal cluster N2 by two conserved consecutive cysteines (possibly allowing its protonation) and the location of essential for activity Tyr87 in Nqo4 (*T. thermophilus* nomenclature) close to N2 and exposed to the Q-binding cavity (*12*). In support of the second model, the overall architecture of the complex strongly suggests a requirement for long-range communication within the enzyme, since the two antiporter-like subunits NuoL and NuoM, likely to be involved in proton pumping, are located about 100 Å away from the hydrophilic domain and the electron transfer pathway (*22, 27*−*29*). Since the 1980s, a range of studies with bovine and *E. coli* enzymes have suggested that significant conformational changes occur upon NAD(P)H or inhibitor (rotenone) binding to complex I (*30*−*34*). Incubation of both bovine (*31*) and *E. coli* enzymes (*34*) with NAD(P)H, but not with $NAD(P)^+$, abolished a number of intersubunit cross-links created by "zero-length" (no spacer arm) reagent EEDQ and also led to increased susceptibility of a number of bovine complex I subunits to tryptic degradation (*32*). Rotenone binding to the bovine enzyme prevented the formation of many cross-links between hydrophilic subunits (*30*). Kinetic studies with the bovine enzyme indicate that NADH binding to the complex results in a conformational change at the ubiquinone-binding site, greatly increasing its affinity toward hydrophobic substrates and inhibitors (*33*). Our recent EM reconstructions of intact *E. coli* complex in the presence of either NAD^+ or NADH suggest that any differences in the conformation are rather small, below current resolution limits of about 35 Å (*35*). Throughout, by "intact complex I" we mean an entire complex purified in detergent, as opposed to isolated peripheral or membrane domain.

The ultimate test on the nature of these conformational changes would be comparison of the atomic structures of the intact complex in the presence of NADH, NAD^+, and inhibitors. High-resolution structural studies are currently possible only with the isolated hydrophilic domain of *T. thermophilus* complex I. However, it is possible that conformational changes observed in the intact enzyme are part of a cooperative, highly regulated process and so they may not occur (or be less pronounced) in the isolated domain. Therefore, we compared patterns of cross-linking of hydrophilic subunits in the presence of NAD^+/NADH for intact *E. coli* complex I and for purified hydrophilic domains of the *E. coli* and *T. thermophilus* enzymes. The patterns were similar in all cases, indicating that conformational changes involving the hydrophilic domain are likely to be similar to those occurring in the intact complex. Further studies on the cross-linking of hydrophobic subunits in intact *E. coli* enzyme revealed that addition of NADH changes the interface of subunits NuoA and NuoJ in the membrane domain, demonstrating long-range communications within the complex. Unexpectedly, addition of NADH also resulted in oxygen-dependent cross-linking and fragmentation of several subunits.

EXPERIMENTAL PROCEDURES

Materials. All detergents were purchased from Glycon (Luckenwalde, Germany). Chromatography columns and instrumentation were from Amersham Biosciences (Uppsala, Sweden) except BioScale DEAE and UNO Q-12 columns from Bio-Rad (Hemel Hampstead, U.K.). Cross-linkers were from Pierce Perbio Science (Tattenhall, U.K.), Complete protease inhibitor tablets from Roche Diagnostics (Lewes, U.K.), and all other chemicals from Sigma (Poole, U.K.).

Protein Purification. The hydrophilic domain (peripheral arm) of complex I from *T. thermophilus* and intact complex I from *E. coli* were purified as described in refs *4* and *8*, respectively. The hydrophilic domain from *E. coli* was isolated by incubating intact *E. coli* complex I on ice for 5 min with 3 mM NAD^+ and then further incubating for 7 h with 0.4 M $CaCl_2$ before separating the hydrophilic and membrane domains by chromatography on a Mono-Q HR 10/100 ion-exchange column.

Cross-Linking. E. coli complex I (10 mg/mL purified protein in 20 mM Bis-Tris, pH 6.0, 50 mM NaCl, 2 mM $CaCl_2$, 18% glycerol (v/v), and 0.5% *n*-dodecyl β-D-maltoside (DDM, w/v)) was diluted 10-fold in incubation buffer (50 mM Bis-Tris, pH 6.0, 3 mM EDTA, and 0.2% DDM (w/v)) and incubated aerobically (unless stated otherwise) for 2 h at 4 °C in the presence or absence of cross-linkers, nucleotides, and/or other additives. EEDQ (*N*-(ethoxycarbonyl)-2-ethoxy-1,2-dihydroquinoline) was first dissolved to 100 mM in methanol and then diluted to 5 mM in incubation buffer before use. NAD^+, NADH, and NADPH were made as 30 mM stocks in 100 mM Bis-Tris, pH 6.0. All other stocks were prepared in incubation buffer.

Samples of the hydrophilic domain of *T. thermophilus* complex I (1.0 mg/mL) in 100 mM HEPES, pH 7.5, 100 mM NaCl, 2 mM $CaCl_2$ (unless stated otherwise), and 1% *n*-octyl β-D-glucoside (OG, w/v) were incubated aerobically (unless stated otherwise) at 22 °C in the presence or absence of cross-linker EEDQ, nucleotides, and/or other additives. Stocks of nucleotides were prepared in 100 mM HEPES, pH 7.5. EEDQ was first dissolved to 100 mM in methanol and then diluted to 5 mM in 100 mM HEPES, pH 7.5, prior to addition to samples.

Concentrations of cross-linkers were optimized so as to avoid the formation of protein aggregates. Complex I was added last to the reaction mixtures. Following incubation with cross-linkers, the reactions were stopped by adding an equal volume of SDS−PAGE sample buffer, which contained 250

mM Tris-HCl, pH 9.15, 40% sucrose (w/v), 4% SDS (w/v), and 50 mM DTT. The samples were analyzed by SDS−PAGE, followed by immunodetection with antibodies against specific *E. coli* and *T. thermophilus* complex I subunits, kindly provided by Drs. T. Yagi and E. Nakamaru-Ogiso (Scripps, La Jolla, CA). Subunit Nqo4 from *T. thermophilus* was detected with antibody against the homologous 49 kDa subunit from *Neurospora crassa*, kindly provided by Dr. U. Schulte (University of Dusseldorf, Germany).

Anaerobic incubations were performed in a Belle Technologies glovebox with an oxygen content below 10 ppm during experiments. All solutions were left for at least 1 h in the glovebox prior to use to ensure they were oxygen free.

Analytical Methods. Protein concentration was measured using the Pierce bicinchoninic acid (BCA) protein assay according to manufacturer's instructions. SDS−PAGE was performed with preprepared Tris−glycine polyacrylamide gels (Invitrogen, Paisley, U.K.) containing a 4−20% acrylamide gradient (w/v), according to the manufacturer's instructions. Unless otherwise stated, all *T. thermophilus* samples were boiled for 3 min in a thermoblock set at 105 °C, immediately before loading onto the gels. Protein bands were visualized by Coomassie Blue R250 or silver staining according to standard protocol. Western blotting was performed using an Invitrogen Xblot-II module at 22 °C for a period of 240 min with 10 mM $NaHCO_3$, 3 mM Na_2CO_3, and 0.01% SDS (w/v), to ensure full transfer of all subunits.

The MagicMark molecular mass standards (Invitrogen) were used to ensure accurate alignment of Western blots for different subunits. Immunodetection was performed using anti-rabbit Ig-HRP and the ECL kit according to manufacturer's instructions (Amersham Biosciences).

RESULTS

Comparison of Cross-Linking Patterns for Intact Complex I and Isolated Hydrophilic Domains. Previously, the cross-linking reagent EEDQ was particularly useful in studies of subunit interactions in complex I (*31, 34*). This "zero-length" reagent links carboxyl groups to nucleophilic side chains of polypeptides which are in direct contact with each other. Control experiments with all the preparations used here have shown that, after cross-linking, protein complexes remain monomeric on a gel filtration column, and so cross-links do not involve more than one assembly (either intact enzyme or hydrophilic domain). First, we verified our previous observations with the intact *E. coli* complex using newly available antibodies against most of the *E. coli* subunits. As shown previously (*34*), for each of subunits NuoB (25 kDa), NuoI (21 kDa), and NuoCD (69 kDa, subunits NuoC and NuoD are fused in *E. coli*), multiple cross-linked products are formed in controls or in the presence of NAD^+. However, these cross-links do not form when NADH is present in samples (Figure 1A). A similar pattern was now observed for NuoE (19 kDa), with a higher molecular mass product (∼120 kDa) likely involving NuoCD (seen as a faint band in NuoCD blot) and possibly NuoF (this antibody was less specific, and so data are less clear and are not shown). The NuoCD cross-linking product at about 100 kDa may involve a hydrophobic subunit (such as NuoH), as there are no clear cross-reacting bands in blots for hydrophilic subunits. A model of the relative arrangement of subunits in bacterial complex I is shown in Figure 1B. One of the major cross-linking products was NuoB + NuoI (∼45 kDa), indicated by an arrow in Figure 1. Subunit NuoG did not form any cross-links in the presence of EEDQ (data not shown). Interestingly, cross-links were abolished not only in the presence of NADH but also when dithionite or DTT was added (lanes 5 and 6 in NuoB and NuoI panels, Figure 1A). This indicates that reduction of complex I with these reducing agents alone could be sufficient to elicit conformational change similar to the one induced by NADH.

As mentioned, currently high-resolution crystallography is possible only with isolated hydrophilic domain of complex I from *T. thermophilus* (*17*). Therefore, we studied cross-linking under similar conditions as above but using the isolated hydrophilic domain instead of intact complex I. As shown in Figure 1C, the purified hydrophilic domain of complex I from *E. coli* shows a similar pattern to the intact enzyme; the major NuoB + NuoI cross-linking product (indicated by an arrow) is not seen in the presence of NADH. Some of the higher molecular mass cross-linking products seen with the intact complex are absent when the hydrophilic domain is used in isolation and so may involve hydrophobic subunits. In the presence of NADH subunit NuoB forms a cross-linking product with NuoCD at about 130 kDa (Figure 1C and a similar, but very faint, band in Figure 1A). Unexpectedly, this product is formed also in the absence of any chemical cross-linkers, as the result of oxidative damage (see below).

Incubation of the isolated hydrophilic domain of complex I from *T. thermophilus* with EEDQ revealed a similar pattern; several cross-links involving subunits Nqo2 (analogue of *E. coli* NuoE), Nqo4 (NuoD), Nqo6 (NuoB), and Nqo9 (NuoI) were formed in controls and with NAD^+, but not when NADH was present (Figure 2). The major products were a Nqo6 + Nqo9 cross-link at about 40 kDa and a Nqo4 + Nqo9 cross-link at about 95 kDa (indicated by arrows in Figure 2). The Nqo4 + Nqo9 cross-link could also involve subunit Nqo15 (no analogue in *E. coli*; data not shown due to low specificity of Nqo15 antibody). Subunit Nqo2 could also be involved in this cross-link, but the Nqo2 band at about 95−100 kDa usually appeared slightly misaligned with Nqo4 and Nqo9 bands, and so that is not conclusive. Subunits Nqo1 (NuoF), Nqo3 (NuoG), and Nqo5 (NuoC) did not form EEDQ-mediated cross-links (data not shown). The similarity of cross-linking patterns between the intact *E. coli* complex and the isolated hydrophilic domains of the *E. coli* and *T. thermophilus* enzymes (Figure 1A vs Figures 1C and 2) indicates that any conformational changes involving hydrophilic subunits, which occur in the intact enzyme, are likely also to occur in the isolated hydrophilic domain. As seen with the *E. coli* enzyme, oxidative damage was observed in the presence of NADH, resulting in cross-linking and protein degradation of subunits Nqo4, Nqo6, and Nqo9 (Figure 2 and below). Consistent with observations with the *E. coli* enzyme (Figure 1A), the addition of dithionite to the *T. thermophilus* enzyme was sufficient to prevent chemical cross-linking, but it did not lead to oxidative damage (Figure 2).

Cross-Linking of Hydrophobic Subunits. Using intact *E. coli* complex I and newly available antibodies against most of the hydrophobic subunits, we extended the cross-linking studies into the hydrophobic domain. Subunit NuoK did

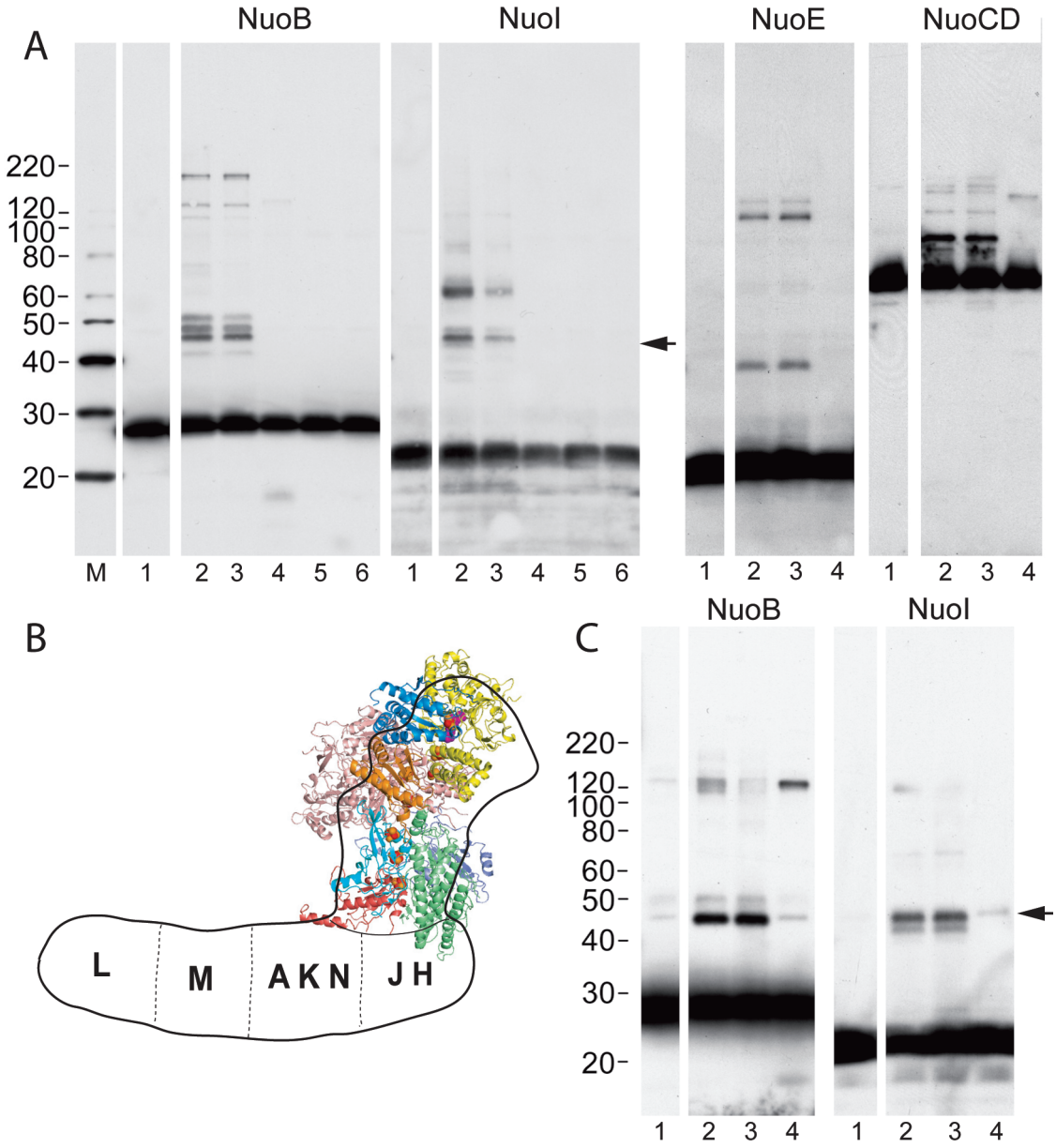

FIGURE 1: Cross-linking of *E. coli* complex I preparations with the zero-length cross-linker EEDQ. (A) Intact complex. (C) Isolated hydrophilic domain. Protein samples were incubated for 2 h at 4 °C with 0.5 mM EEDQ and analyzed by SDS−PAGE followed by immunodetection with antibodies against indicated subunits. Lane 1, control without cross-linker; lane 2, cross-linker only; lane 3, cross-linker and 3 mM NAD^+; lane 4, cross-linker and 3 mM NADH; lane 5, cross-linker and 10 mM sodium dithionite; lane 6, cross-linker and 2 mM DTT. Lane M contained molecular mass markers with sizes shown on the left. Arrows indicate the major cross-linking product of subunits NuoB + NuoI. (B) Arrangement of subunits in bacterial complex I (adapted from ref *12*). Letters indicate Nuo subunits of the membrane domain (*E. coli* nomenclature). The hydrophilic domain is represented by the structure of the *T. thermophilus* domain (PDB 2FUG), with subunits colored similarly to ref *17*: Nqo6 (NuoB), red; Nqo4 (NuoD), green; Nqo5 (NuoC), violet; Nqo9 (NuoI), cyan; Nqo3 (NuoG), salmon; Nqo15, orange; Nqo1 (NuoF), yellow; Nqo2 (NuoE), blue.

not show any cross-links, but subunits NuoA (16 kDa) and NuoJ (20 kDa) formed a cross-linking product at about 35 kDa (indicated by an arrow in Figure 3A). It was detected when either EEDQ or EDC (1-ethyl-3-(3-dimethylaminopropyl)carbodiimide hydrochloride), another zero-length cross-linking agent coupling carboxyl groups to primary amines, was used. This observation indicates that in the membrane domain subunits NuoA and NuoJ are in close contact to each other. When EEDQ was used, the cross-link was absent when NADH was added (Figure 3), in a pattern similar to that seen with the hydrophilic subunits (Figures 1 and 2). Therefore, a conformational change involving hydrophilic subunits is likely to extend into the membrane domain, at least to the interface with the hydrophilic domain, where subunits NuoA and NuoJ are likely located (Figure 1B). The observation that the cross-links with EDC (having different specificity from EEDQ) were still present when the enzyme was incubated with NADH would be consistent with our current view that conformational changes are rather small and specific, although likely to be long range (*35*).

The two largest hydrophobic subunits NuoL (66 kDa) and NuoM (57 kDa) did not form any cross-links when zero-length reagents were used. In the presence of sulfo-SMCC (*N*-sulfosuccinimidyl 4-(*N*-maleimidomethyl)cyclohexane-1-carboxylate), with 8.3 Å spacer arm, a possible NuoL + NuoM cross-link was formed, although the antibodies against these subunits were not highly specific and so the cross-

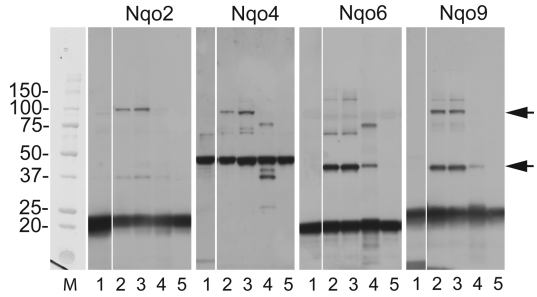

FIGURE 2: Cross-linking of the hydrophilic domain of *T. thermophilus* complex I with the zero-length cross-linker EEDQ. Samples were incubated for 2 h at 22 °C with 0.5 mM EEDQ and analyzed by SDS−PAGE followed by immunodetection with antibodies against indicated subunits. Lane 1, control without cross-linker; lane 2, cross-linker only; lane 3, cross-linker and 3 mM NAD^+; lane 4, cross-linker and 3 mM NADH; lane 5, cross-linker and 5 mM sodium dithionite. Lane M contained molecular mass markers with sizes shown on the left. Arrows indicate cross-linking products of subunits Nqo4 + Nqo9 at about 95 kDa and Nqo6 + Nqo9 at about 40 kDa.

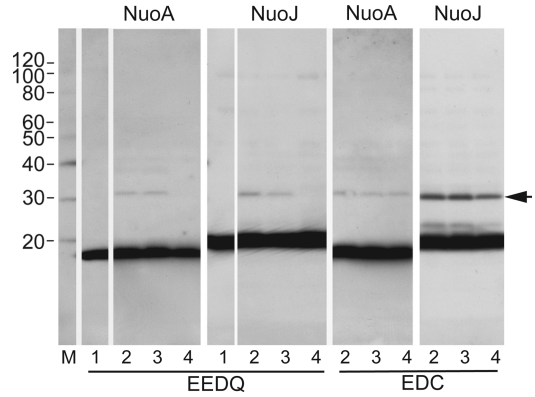

FIGURE 3: Cross-linking of hydrophobic subunits of intact *E. coli* complex I. Samples were incubated for 2 h at 4 °C either with 0.5 mM EEDQ (left) or with 5 mM EDC (right) and analyzed by SDS−PAGE followed by immunodetection with antibodies against subunits NuoA and NuoJ. Lane 1, control without cross-linker; lane 2, cross-linker only; lane 3, cross-linker and 3 mM NAD^+; lane 4, cross-linker and 3 mM NADH. Lane M contained molecular mass markers with sizes shown on the left. Arrow indicates cross-linking product of subunits NuoA + NuoJ.

linked band was rather weak (Figure S1, Supporting Information). The existence of a NuoL/NuoM interface is consistent with the current model of complex I (Figure 1B). The cross-linking pattern did not change in the presence of NADH. However, since only a zero-length cross-linker normally reveals such a change (*34*), this observation does not necessarily argue against conformational changes occurring also in the distal part of the membrane domain, where NuoL and NuoM are located (Figure 1B) (*27*). Several conserved charged residues in NuoM and NuoN subunits are essential for the quinone reductase activity of the complex, consistent with long-range interactions being part of the mechanism (*36, 37*).

NADH-Induced, ROS-Dependent, Cross-Linking and Proteolysis of Subunits of Complex I. As mentioned earlier, in the course of these experiments it became apparent that in the presence of NADH, without any chemical cross-linkers, covalent cross-links between several subunits can be formed. In intact *E. coli* complex I, a cross-link between subunits NuoB and NuoCD can be detected at about 130 kDa, indicated by an arrow in Figure 4A. It is formed within 1 h

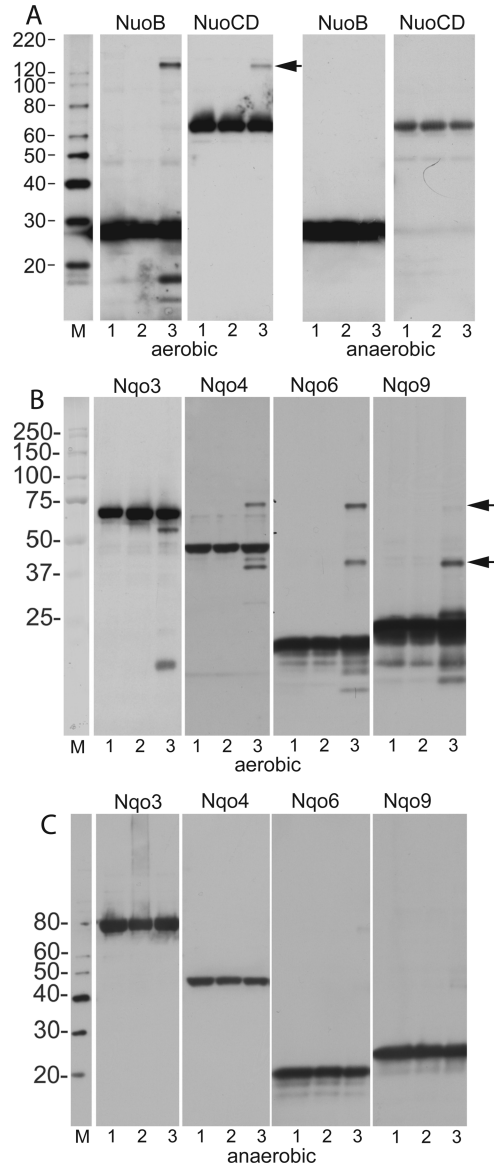

FIGURE 4: NADH-induced, ROS-dependent protein cross-linking and proteolysis. (A) Intact *E. coli* complex I was incubated for 2 h at 4 °C with nucleotides either aerobically (left) or anaerobically (right). Arrow indicates cross-linking product of subunits NuoB + NuoCD. (B, C) The hydrophilic domain of *T. thermophilus* complex I was incubated for 2 h at 22 °C with nucleotides either aerobically (B) or anaerobically (C). Arrows indicate cross-linking products of subunits Nqo4 + Nqo6 at about 75 kDa and subunits Nqo6 + Nqo9 at about 40 kDa. Samples were analyzed by SDS−PAGE followed by immunodetection with antibodies against indicated subunits. Lane 1, control with no additions; lane 2, 3 mM NAD^+; lane 3, 3 mM NADH. Lane M contained molecular mass markers with sizes shown on the left.

of incubation at 4 °C and slowly accumulates during prolonged incubation. In parallel, degradation of subunit NuoB is observed, as evidenced by the accumulation of small molecular mass bands cross-reacting with the antibody (Figure 4A, left panel). The apparent molecular mass of the cross-linking product is somewhat higher than the expected sum of NuoB/NuoCD (94 kDa), which could be due to aberrant behavior during SDS−PAGE as a result of the presence of an intersubunit cross-link(s). Other subunits do not appear to be involved in this product, as there are no other cross-reacting bands in blots for hydrophilic subunits, and a similar cross-linking product is present in isolated

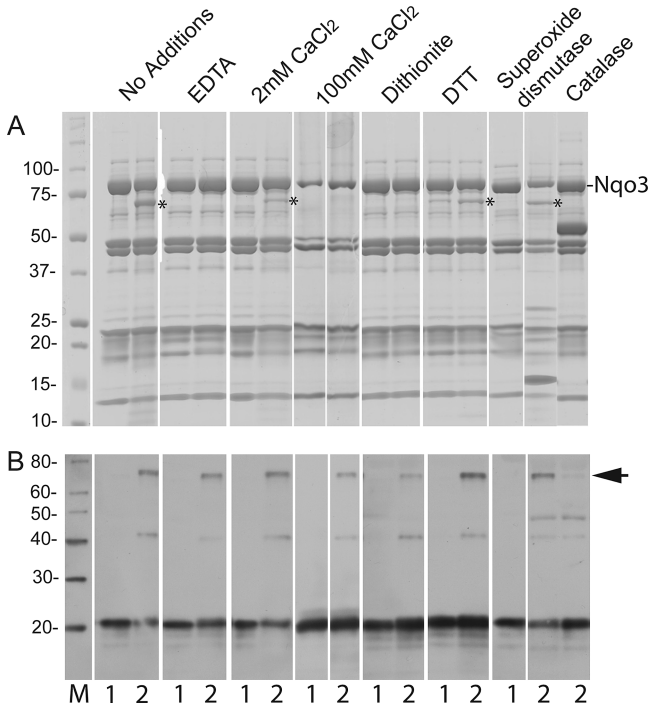

FIGURE 5: The nature of NADH-induced, ROS-dependent protein cross-linking and proteolysis. The hydrophilic domain of *T. thermophilus* complex I was incubated for 6 h at 22 °C with (or without) NADH and additions as indicated. Standard 2 mM $CaCl_2$ was omitted from "no additions" and "EDTA" samples. Where indicated, 5 mM EDTA, 5 mM sodium dithionite, 5 mM DTT, 2500 units of superoxide dismutase, and 0.5 mg/mL catalase were present. (A) Coomassie blue stained gel. Stars indicate the product of proteolysis of subunit Nqo3. (B) Immunodetection of the blot of the gel similar to (A) with antibody against subunit Nqo6. Arrow indicates cross-linking product of subunits Nqo4 + Nqo6. Lane 1, control without nucleotides; lane 2, 3 mM NADH added.

hydrophilic domain devoid of hydrophobic subunits (Figure 1C). Similarly, when the isolated hydrophilic domain of *T. thermophilus* complex I was used, in the presence of NADH a cross-link between Nqo4 (NuoD analog) and Nqo6 (NuoB) was observed (upper arrow in Figure 4B), as well as between Nqo6 and Nqo9 (lower arrow). In this case, both cross-linking products had expected molecular masses (Figure 4B). In addition, degradation of these three subunits, as well as Nqo3, was observed (Figure 4B). Previously, using Coomassie-stained gels, we observed degradation of subunit NuoG (Nqo3 analogue) in *E. coli* complex I (*34*), although this was attributed to a contaminating protease at the time. When similar experiments were repeated under anaerobic conditions, cross-linking and degradation were completely prevented, both in *E. coli* (Figure 4A, right panel) and in *T. thermophilus* (Figure 4C). Proteolysis of subunit NuoG in *E. coli* was also prevented (not shown). This complete dependence on oxygen suggests that ROS, known to be generated by complex I in the presence of NADH (*10, 38*), are responsible for the observed cross-linking and proteolysis.

To study the nature of NADH-induced cross-linking and degradation further, we used as representative reactions the proteolysis of *T. thermophilus* subunit Nqo3 and cross-linking of subunit Nqo6. The degree of degradation of Nqo3 (86 kDa) into a smaller fragment of about 70 kDa (indicated by stars in Figure 5A) was greatest in the buffer without any added metals or chelators ("no additions" in Figure 5A). Appearance of this fragment is accompanied by a decrease in the amount of native Nqo3, as can be seen from the comparison of control and NADH-containing lanes. Addition of chelator EDTA prevented proteolysis, consistent with our previous observations on *E. coli* complex (*34*). This indicates that oxidative proteolysis of Nqo3 requires the presence of low amounts of metal ions, carried over with the protein sample. Upon addition of 2 mM $CaCl_2$ proteolysis was somewhat diminished, possibly reflecting stabilization of the hydrophilic domain, observed previously with the *E. coli* complex (*8*). Proteolysis was not detected at very high concentrations of divalent cations, although in this case some aggregation of protein occurred during SDS−PAGE, as evidenced by a diffuse high molecular mass smear and substoichiometric amounts of subunits Nqo3 and Nqo1 (100 mM $CaCl_2$ lanes in Figure 5A). The reducing agent dithionite, but not DTT, prevented degradation. Dithionite is also an oxygen scavenger and a chelator, which probably explains its effect. Superoxide dismutase (SOD) had no effect on degradation, while catalase fully prevented it. This indicates that the damaging species is not superoxide but, instead, hydrogen peroxide or its products. In any case, under our experimental conditions any superoxide generated by complex I likely dismutates quickly to peroxide, since superoxide dismutase does not have a significant effect on the rate of hydrogen peroxide production in an Amplex Red assay (data not shown). The most likely species involved in oxidative damage is not hydrogen peroxide itself but highly reactive hydroxyl radicals, which can not only modify protein side chains (like peroxide) but also lead to protein degradation and cross-linking (*39, 40*). Hydroxyl radicals can be produced by the Fenton reaction between reduced transition metals (often this is iron(II)) and hydrogen peroxide (*40, 41*). The prevention of degradation by EDTA (Figure 5A and (*34*)) is consistent with this proposal.

Interestingly, EDTA did not prevent NADH-induced cross-links, at least not those between subunits Nqo4 and Nqo6 (Figure 5B). This suggests that some local, nonchelatable metal may be available for the Fenton reaction. The terminal, high-potential Fe-S cluster N2 is coordinated at the interface of subunits Nqo4 and Nqo6 and could be the source of iron for this reaction. Dithionite diminishes, but does not fully prevent, cross-links, while catalase is more effective (Figure 5B). This indicates that at least part of the effect of dithionite in preventing degradation (Figure 5A) may be due to its chelating properties.

NADPH can be a substrate for complex I, albeit a poor one (about 1−2% of activity with NADH; data not shown), and it can reduce Fe-S clusters of complex I (*42*). Consistently, we observed similar proteolysis and ROS-dependent cross-linking effects when NADPH was used instead of NADH (not shown).

NADH-Induced, ROS-Dependent, Destabilization of the Hydrophilic Domain of Complex I from T. thermophilus. The hydrophilic domain of *T. thermophilus* complex I is remarkably stable and requires boiling for several minutes in order to be disrupted in SDS solutions (*4*), which was done for all SDS gels containing *T. thermophilus* samples shown so far. However, prolonged incubation in NADH under aerobic conditions leads to destabilization of the complex, so that after 3 h most of the complex could be disrupted by SDS at room temperature, without preboiling of the sample (Figure 6A). Note how disappearance of the intact domain, indicated

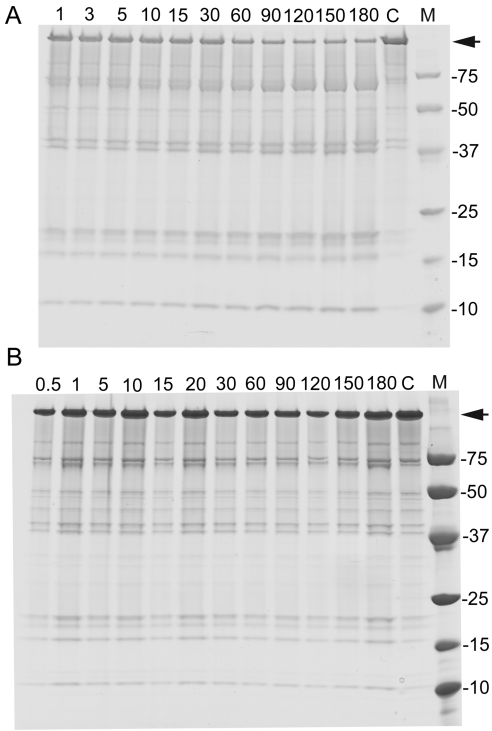

FIGURE 6: Destabilization (sensitization to SDS) of the hydrophilic domain of *T. thermophilus* complex I in the presence of NADH and oxygen. (A) Aerobic incubation. (B) Anaerobic incubation. Samples, containing 100 mM $CaCl_2$, were incubated at 22 °C with 3 mM NADH for times indicated in minutes and then subjected to SDS−PAGE, without boiling prior to loading on the gel. Arrow indicates intact hydrophilic domain. Lane C is a control sample incubated for 3 h without NADH under identical conditions. Lane M contained molecular mass markers with sizes shown on the right.

by an arrow, is accompanied by an increase in the amounts of individual subunits. The half-time of this process was about 1 h, as indicated by densitometry analysis of the gels (not shown). However, under anaerobic conditions destabilization was prevented (note similar amounts of intact domain throughout Figure 6B). This suggests that ROS are responsible for this process as well, although it does not appear to be a simple consequence of proteolysis shown in Figures 4 and 5. After a 2 h aerobic incubation most of the protein becomes sensitive to SDS (Figure 6A), while under similar conditions (100 mM $CaCl_2$ in the buffer) there is no visible degradation of subunit Nqo3 and only minor degradation of other subunits (data not shown). High concentration of Ca^{2+} in these experiments was present in order to mimic our crystallization conditions. With 2 mM $CaCl_2$ in the buffer (as mostly used throughout, including Figure 4) the observations were similar to those shown in Figure 6; i.e., most of protein becomes sensitive to SDS after 2 h incubation with NADH (data not shown). However, in this case also, the proteolysis of subunits still involved only a minor proportion of total protein (Figure 4B). Thus, it appears that, apart from protein degradation, some other oxidative damage contributes to the observed destabilization. Incubation of the hydrophilic domain with the NADH/NAD^+ mixture in a range of ratios, thus varying applied redox potential between −400 and −270 mV, followed by SDS−PAGE and densitometry analysis, suggests that the midpoint redox potential for the destabilization process is about −320 mV (Figure S2, Supporting Information). This value roughly coincides with the two-electron midpoint redox potential of complex I-bound flavin (*43*), which suggests that reduction of flavin (rather than, for example, of high potential cluster N2) may be necessary for destabilization to occur.

It has to be noted that the domain is still perfectly stable under similar conditions in octyl glucoside (used during crystallization) or other mild detergents (as judged from gel filtration chromatography; data not shown). Data in Figures 4 and 6 suggest that crystallization of complex I in the presence of NADH should be done under strictly anaerobic conditions, to avoid any oxidative damage. Exposure of crystals to air during harvesting/freezing should also be minimized and kept within approximately 30 min (Figure 6). Interestingly, high concentrations of divalent cations, which seem to stabilize *T. thermophilus* hydrophilic domain somewhat (Figure 5), are also necessary for crystallization (*17*).

DISCUSSION

A range of studies previously indicated that complex I likely undergoes conformational change in the presence of NADH (or NADPH), compared to control (oxidized) samples (as purified or with $NAD(P)^+$ added) (*30*−*34*). Along with limited proteolysis (*32*) and kinetic data (*33*), chemical cross-linking was instrumental in revealing these changes (*30, 31, 34*). Zero-length cross-linkers without a spacer arm, such as EEDQ, were especially useful, presumably because any changes in the structure are smaller than the linker length in other reagents used (about 8−10 Å). This is consistent with our recent cryo-EM data showing that any conformational changes are smaller than the current resolution of EM maps (*35*). As noted in the introduction, one of the two discussed mechanisms of coupling between electron transfer and proton translocation in complex I involves long-range conformational changes in the enzyme. Here we have shown that the isolated hydrophilic domain from either *E. coli* or *T. thermophilus* complex I behaves similarly to the intact enzyme in the presence of EEDQ; many cross-linking products which are present in the oxidized samples are absent when the domain is reduced by NADH (Figures 1 and 2). This is important since currently only the isolated hydrophilic domain from *T. thermophilus* can be used for comparison of oxidized and reduced structures at high resolution by X-ray crystallography. Cross-linking data indicate that any conformational changes occurring in the intact complex during reduction (perhaps as part of the catalytic cycle) are likely to be preserved in the isolated hydrophilic domain. Of course, the possibility still remains that some of the finer redox-linked changes in the structure of hydrophilic subunits require interaction with the membrane domain and so will occur only in an intact, fully active enzyme. This can be verified only when the structure of the entire enzyme is determined. However, our cross-linking data suggest that the structure of the NADH-reduced isolated hydrophilic domain should provide a good starting point for discussion of the coupling mechanism of complex I and any related conformational changes.

Importantly, reducing agents dithionite and DTT prevented the formation of EEDQ-mediated cross-links, similarly to NADH (Figures 1A and 2). Therefore, it appears that conformational changes involving subunits Nqo2 (NuoE),

Nqo4 (NuoCD), Nqo6 (NuoB), and Nqo9 (NuoI), as detected by cross-linking, are mainly the result of the reduction of the enzyme and its Fe−S clusters and are not caused by NADH binding *per se*.

Our observation that, in intact *E. coli* complex I, hydrophobic subunits NuoA and NuoJ can be cross-linked by "zero-length" reagents and so are in close contact to each other is consistent with our model for subunit arrangement in the projection map of the membrane domain (*29*). It is also consistent with the proposal, based on mutagenesis studies, that subunits NuoK, NuoA, and NuoJ may form at their interface a multihelix bundle involved in a proton translocation mechanism (*44*). Importantly, the cross-link between subunits NuoA and NuoJ was prevented in the presence of NADH, confirming that redox-linked conformational changes in complex I extend into the membrane domain, at least to the area of the interface with the peripheral arm, where these subunits are located (*22, 29, 45*).

A surprising discovery was the fact that NADH can induce intersubunit cross-links without any added chemical cross-linkers. As shown clearly in Figure 4, this process is strictly dependent on the presence of oxygen, so it must be mediated by ROS produced by complex I in the presence of NADH. Our preliminary studies (data not shown) indicate that in the presence of NADH our preparations of *E. coli* complex I and of the hydrophilic domain of *T. thermophilus* enzyme generate hydrogen peroxide and/or superoxide at rates in the range of those previously published for bovine and *E. coli* enzymes (*38, 46, 47*). Further investigation (Figure 5) suggests that the most likely species causing cross-linking and proteolysis are hydroxyl radicals produced from hydrogen peroxide by the Fenton reaction.

Flavin is now generally regarded as a main source of ROS in complex I (*12, 38, 46, 48, 49*), although (semi)quinone (*50, 51*) and cluster N2 (*52*) are also being discussed. There could be two possibilities why the Nqo6/Nqo4 (NuoB/NuoCD) interface is the most susceptible to NADH-induced cross-linking in both *E. coli* and *T. thermophilus* (Figure 4). First, it is possible that hydrogen peroxide produced at the flavin site (or near it by dismutation of superoxide) is converted to hydroxyl radical at the interface of these two subunits, where [4Fe-4S] cluster N2 is located. In the hydrophilic domain, this cluster is shielded from the solvent, but it is still close to the solvent- (or membrane *in vivo*) exposed cavity containing the quinone-binding site (*17*). Two of the iron atoms in this cluster are coordinated by a unique tandem cysteine motif, which leads to unfavorable geometry, weakened $Fe-S^{Cys}$ bonds, and in a reduced state may leave iron partially free for the Fenton reaction. The fact that the Nqo4-Nqo6 cross-link still forms in the presence of EDTA (Figure 4B), which prevents proteolysis of Nqo3 (Figure 4A), is consistent with this proposal, since cluster N2 iron would be nonchelatable. A second possibility is that even though most of ROS are produced at the flavin site, as suggested by the structure of the site and a wide range of data (*12*), some proportion could also be produced at cluster N2. This cluster would be fully reduced by NADH due to its high potential, and any hydrogen peroxide produced at or near this site may be converted to hydroxyl radical locally. Since the *Yarrowia lipolytica* complex I mutant with (presumably) strongly lowered potential of cluster N2 did not show any change in ROS production (*48*), the first scenario out of the two could be more likely, although further studies are needed to differentiate the possibilities.

Most subunits susceptible to NADH-induced proteolysis are also near cluster N2 (Nqo4, Nqo6, and Nqo9), except for subunit Nqo3 (NuoG). This subunit has a very large exposed C-terminal domain, which is flexible at the surface of its tip (high *B*-factors in the structure (*17*)), and so it may be particularly vulnerable to ROS damage. The *E. coli* NuoCD subunit seems more susceptible to NADH-induced proteolysis in the isolated hydrophilic domain, rather than in the intact complex I (data not shown), possibly because areas prone to oxidative damage are shielded by the membrane domain.

Generally, when ROS damage to complex I *in vivo* is discussed, mostly side-chain modifications, such as oxidation or glutathionylation of sulfhydryl groups, are considered (*53, 54*). Our data suggest that, along with such reversible modifications, irreversible proteolysis and cross-linking should also be considered as potential consequences of oxidative damage *in vivo*.

ACKNOWLEDGMENT

We thank Drs. T. Yagi and E. Nakamaru-Ogiso (Scripps, La Jolla, CA) for a kind gift of antibodies against subunits of complex I from *E. coli* and *T. thermophilus*.

SUPPORTING INFORMATION AVAILABLE

Figure S1, cross-linking of *E. coli* NuoL and NuoM subunits by sulfo-SMCC; Figure S2, stability of the hydrophilic domain of *T. thermophilus* complex I in SDS at different redox potentials set by the NAD^+/NADH ratio. This material is available free of charge via the Internet at http://pubs.acs.org.

REFERENCES

1. Walker, J. E. (1992) The NADH-ubiquinone oxidoreductase (complex I) of respiratory chains. *Q. Rev. Biophys. 25*, 253–324.
2. Yagi, T., and Matsuno-Yagi, A. (2003) The proton-translocating NADH-Quinone oxidoreductase in the respiratory chain: the secret unlocked. *Biochemistry 42*, 2266–2274.
3. Carroll, J., Fearnley, I. M., Skehel, J. M., Shannon, R. J., Hirst, J., and Walker, J. E. (2006) Bovine complex I is a complex of 45 different subunits. *J. Biol. Chem. 281*, 32724–32727.
4. Hinchliffe, P., Carroll, J., and Sazanov, L. A. (2006) Identification of a novel subunit of respiratory complex I from *Thermus thermophilus*. *Biochemistry 45*, 4413–4420.
5. Grigorieff, N. (1998) Three-dimensional structure of bovine NADH: ubiquinone oxidoreductase (complex I) at 22 Å in ice. *J. Mol. Biol. 277*, 1033–1046.
6. Peng, G., Fritzsch, G., Zickermann, V., Schagger, H., Mentele, R., Lottspeich, F., Bostina, M., Radermacher, M., Huber, R., Stetter, K. O., and Michel, H. (2003) Isolation, characterization and electron microscopic single particle analysis of the NADH:ubiquinone oxidoreductase (complex I) from the hyperthermophilic eubacterium *Aquifex aeolicus*. *Biochemistry 42*, 3032–3039.
7. Guenebaut, V., Schlitt, A., Weiss, H., Leonard, K., and Friedrich, T. (1998) Consistent structure between bacterial and mitochondrial NADH:ubiquinone oxidoreductase (complex I). *J. Mol. Biol. 276*, 105–112.
8. Sazanov, L. A., Carroll, J., Holt, P., Toime, L., and Fearnley, I. M. (2003) A role for native lipids in the stabilization and two-dimensional crystallization of the *Escherichia coli* NADH-ubiquinone oxidoreductase (complex I). *J. Biol. Chem. 278*, 19483–19491.
9. Schapira, A. H. (1998) Human complex I defects in neurodegenerative diseases. *Biochim. Biophys. Acta 1364*, 261–270.
10. Balaban, R. S., Nemoto, S., and Finkel, T. (2005) Mitochondria, oxidants, and aging. *Cell 120*, 483–495.

11. Dawson, T. M., and Dawson, V. L. (2003) Molecular pathways of neurodegeneration in Parkinson's disease. *Science 302*, 819–822.
12. Sazanov, L. A. (2007) Respiratory complex I: mechanistic and structural insights provided by the crystal structure of the hydrophilic domain. *Biochemistry 46*, 2275–2288.
13. Hofhaus, G., Weiss, H., and Leonard, K. (1991) Electron microscopic analysis of the peripheral and membrane parts of mitochondrial NADH dehydrogenase (complex I). *J. Mol. Biol. 221*, 1027–1043.
14. Radermacher, M., Ruiz, T., Clason, T., Benjamin, S., Brandt, U., and Zickermann, V. (2006) The three-dimensional structure of complex I from *Yarrowia lipolytica*: a highly dynamic enzyme. *J. Struct. Biol. 154*, 269–279.
15. Ohnishi, T. (1998) Iron-sulfur clusters/semiquinones in complex I. *Biochim. Biophys. Acta 1364*, 186–206.
16. Hinchliffe, P., and Sazanov, L. A. (2005) Organization of iron-sulfur clusters in respiratory complex I. *Science 309*, 771–774.
17. Sazanov, L. A., and Hinchliffe, P. (2006) Structure of the hydrophilic domain of respiratory complex I from *Thermus thermophilus*. *Science 311*, 1430–1436.
18. Fearnley, I. M., and Walker, J. E. (1992) Conservation of sequences of subunits of mitochondrial complex I and their relationships with other proteins. *Biochim. Biophys. Acta 1140*, 105–134.
19. Kikuno, R., and Miyata, T. (1985) Sequence homologies among mitochondrial DNA-coded URF2, URF4 and URF5. *FEBS Lett. 189*, 85–88.
20. Mathiesen, C., and Hagerhall, C. (2003) The "antiporter module" of respiratory chain complex I includes the MrpC/NuoK subunit—a revision of the modular evolution scheme. *FEBS Lett. 549*, 7–13.
21. Dutton, P. L., Moser, C. C., Sled, V. D., Daldal, F., and Ohnishi, T. (1998) A reductant-induced oxidation mechanism for complex I. *Biochim. Biophys. Acta 1364*, 245–257.
22. Holt, P. J., Morgan, D. J., and Sazanov, L. A. (2003) The location of NuoL and NuoM subunits in the membrane domain of the *Escherichia coli* complex I: implications for the mechanism of proton pumping. *J. Biol. Chem. 278*, 43114–43120.
23. Friedrich, T. (2001) Complex I: a chimaera of a redox and conformation-driven proton pump? *J. Bioenerg. Biomembr. 33*, 169–177.
24. Brandt, U. (2006) Energy converting NADH:quinone oxidoreductase (complex I). *Annu. Rev. Biochem. 75*, 69–92.
25. Sazanov, L. A., Peak-Chew, S. Y., Fearnley, I. M., and Walker, J. E. (2000) Resolution of the membrane domain of bovine complex I into subcomplexes: implications for the structural organization of the enzyme. *Biochemistry 39*, 7229–7235.
26. Sherwood, S., and Hirst, J. (2006) Investigation of the mechanism of proton translocation by NADH:ubiquinone oxidoreductase (complex I) from bovine heart mitochondria: does the enzyme operate by a Q-cycle mechanism? *Biochem. J. 400*, 541–550.
27. Baranova, E. A., Morgan, D. J., and Sazanov, L. A. (2007) Single particle analysis confirms distal location of subunits NuoL and NuoM in *Escherichia coli* complex I. *J. Struct. Biol. 159*, 238–242.
28. Sazanov, L. A., and Walker, J. E. (2000) Cryo-electron crystallography of two sub-complexes of bovine complex I reveals the relationship between the membrane and peripheral arms. *J. Mol. Biol. 302*, 455–464.
29. Baranova, E. A., Holt, P. J., and Sazanov, L. A. (2007) Projection structure of the membrane domain of *Escherichia coli* respiratory complex I at 8 Å resolution. *J. Mol. Biol. 366*, 140–154.
30. Gondal, J. A., and Anderson, W. M. (1985) The molecular morphology of bovine heart mitochondrial NADH-ubiquinone reductase. Native disulfide-linked subunits and rotenone-induced conformational changes. *J. Biol. Chem. 260*, 12690–12694.
31. Belogrudov, G., and Hatefi, Y. (1994) Catalytic sector of complex I (NADH:ubiquinone oxidoreductase): subunit stoichiometry and substrate-induced conformation changes. *Biochemistry 33*, 4571–4576.
32. Yamaguchi, M., Belogrudov, G. I., and Hatefi, Y. (1998) Mitochondrial NADH-ubiquinone oxidoreductase (complex I). Effect of substrates on the fragmentation of subunits by trypsin. *J. Biol. Chem. 273*, 8094–8098.
33. Hano, N., Nakashima, Y., Shinzawa-Itoh, K., and Yoshikawa, S. (2003) Effect of the side chain structure of coenzyme Q on the steady state kinetics of bovine heart NADH: coenzyme Q oxidoreductase. *J. Bioenerg. Biomembr. 35*, 257–265.
34. Mamedova, A. A., Holt, P. J., Carroll, J., and Sazanov, L. A. (2004) Substrate-induced conformational change in bacterial complex I. *J. Biol. Chem. 279*, 23830–23836.
35. Morgan, D. J., and Sazanov, L. A. (2008) Three-dimensional structure of respiratory complex I from *Escherichia coli* in ice in the presence of nucleotides. *Biochim. Biophys. Acta 1777*, 711–718.
36. Amarneh, B., and Vik, S. B. (2003) Mutagenesis of subunit N of the *Escherichia coli* complex I. Identification of the initiation codon and the sensitivity of mutants to decylubiquinone. *Biochemistry 42*, 4800–4808.
37. Torres-Bacete, J., Nakamaru-Ogiso, E., Matsuno-Yagi, A., and Yagi, T. (2007) Characterization of the NuoM (ND4) subunit in *Escherichia coli* NDH-1: conserved charged residues essential for energy-coupled activities. *J. Biol. Chem. 282*, 36914–36922.
38. Esterhazy, D., King, M. S., Yakovlev, G., and Hirst, J. (2008) Production of reactive oxygen species by complex I (NADH: ubiquinone oxidoreductase) from *Escherichia coli* and comparison to the enzyme from mitochondria. *Biochemistry 47*, 3964–3971.
39. Davies, M. J. (2005) The oxidative environment and protein damage. *Biochim. Biophys. Acta 1703*, 93–109.
40. Sayre, L. M., Moreira, P. I., Smith, M. A., and Perry, G. (2005) Metal ions and oxidative protein modification in neurological disease. *Ann. Ist. Super. Sanita 41*, 143–164.
41. Imlay, J. A. (2008) Cellular defenses against superoxide and hydrogen peroxide. *Annu. Rev. Biochem. 77*, 755–776.
42. Vinogradov, A. D. (1998) Catalytic properties of the mitochondrial NADH-ubiquinone oxidoreductase (complex I) and the pseudo-reversible active/inactive enzyme transition. *Biochim. Biophys. Acta 1364*, 169–185.
43. Sled, V. D., Rudnitzky, N. I., Hatefi, Y., and Ohnishi, T. (1994) Thermodynamic analysis of flavin in mitochondrial NADH: ubiquinone oxidoreductase (complex I). *Biochemistry 33*, 10069–10075.
44. Kao, M. C., Nakamaru-Ogiso, E., Matsuno-Yagi, A., and Yagi, T. (2005) Characterization of the membrane domain subunit NuoK (ND4L) of the NADH-quinone oxidoreductase from *Escherichia coli*. *Biochemistry 44*, 9545–9554.
45. Kao, M. C., Matsuno-Yagi, A., and Yagi, T. (2004) Subunit proximity in the H^+-translocating NADH-quinone oxidoreductase probed by zero-length cross-linking. *Biochemistry 43*, 3750–3755.
46. Kussmaul, L., and Hirst, J. (2006) The mechanism of superoxide production by NADH:ubiquinone oxidoreductase (complex I) from bovine heart mitochondria. *Proc. Natl. Acad. Sci. U.S.A. 103*, 7607–7612.
47. Grivennikova, V. G., and Vinogradov, A. D. (2006) Generation of superoxide by the mitochondrial complex I. *Biochim. Biophys. Acta 1757*, 553–561.
48. Galkin, A., and Brandt, U. (2005) Superoxide radical formation by pure complex I (NADH:ubiquinone oxidoreductase) from *Yarrowia lipolytica*. *J. Biol. Chem. 280*, 30129–30135.
49. Kudin, A. P., Bimpong-Buta, N. Y., Vielhaber, S., Elger, C. E., and Kunz, W. S. (2004) Characterization of superoxide-producing sites in isolated brain mitochondria. *J. Biol. Chem. 279*, 4127–4135.
50. Lambert, A. J., and Brand, M. D. (2004) Inhibitors of the quinone-binding site allow rapid superoxide production from mitochondrial NADH:ubiquinone oxidoreductase (complex I). *J. Biol. Chem. 279*, 39414–39420.
51. Ohnishi, S. T., Ohnishi, T., Muranaka, S., Fujita, H., Kimura, H., Uemura, K., Yoshida, K., and Utsumi, K. (2005) A possible site of superoxide generation in the complex I segment of rat heart mitochondria. *J. Bioenerg. Biomembr. 37*, 1–15.
52. Fato, R., Bergamini, C., Leoni, S., Strocchi, P., and Lenaz, G. (2008) Generation of reactive oxygen species by mitochondrial complex I: implications in neurodegeneration, Neurochem. Res. Epub.
53. Taylor, E. R., Hurrell, F., Shannon, R. J., Lin, T. K., Hirst, J., and Murphy, M. P. (2003) Reversible glutathionylation of complex I increases mitochondrial superoxide formation. *J. Biol. Chem. 278*, 19603–19610.
54. Chen, Y. R., Chen, C. L., Zhang, L., Green-Church, K. B., and Zweier, J. L. (2005) Superoxide generation from mitochondrial NADH dehydrogenase induces self-inactivation with specific protein radical formation. *J. Biol. Chem. 280*, 37339–37348.

BI801160U